Journal of Electroceramics, 13, 697–701, 2004

On the Relationship Between the Grain Size and Gas-Sensitivity of Chemo-Resistive Metal-Oxide Gas Sensors with Nanosized Grains

AVNER ROTHSCHILD* & YIGAL KOMEM

Faculty of Materials Engineering, Technion–Israel Institute of Technology, Haifa 32000, Israel

Submitted February 12, 2003; Revised November 18, 2003; Accepted November 20, 2003

Abstract. In this work we elaborate the effect of grain size on the sensitivity of chemo-resistive metal-oxide gas sensors with nanosized grains. The effective carrier concentration in nanocrystalline SnO_2 sensors with various grain sizes is calculated as a function of the surface state density. This involves numerical computation of the charge balance equation (i.e., the electroneutrality condition) using approximated analytical solutions of Poisson's equation for small spherical crystallites. The calculations demonstrate a sharp decrease in the carrier concentration when the surface state density reaches a critical value that corresponds to a condition of fully depleted grains, namely when nearly all the electrons are trapped at the surface. Assuming that the variations in the surface state density are induced by surface interactions with the gas phase, these calculations enable to simulate the response curves of nanocrystalline SnO_2 gas sensors. The simulations show that the conductivity increases linearly with decreasing trapped charge densities, and that the sensitivity to the gas-induced variations in the trapped charge density is proportional to $1/D$, where D is the average grain size.

Keywords: gas sensors, metal-oxides, grain size, nanocrystalline, SnO_2

1. Introduction

One of the most important factors controlling the sensitivity of chemo-resistive metal-oxide gas sensors is the grain size (D) [1–3]. It was found that the sensitivity is enhanced considerably when D becomes smaller than $2L$, where L is the width of the space-charge (depletion) region that is produced at the surface of the crystallites due to chemisorbed adions [4]. This paper presents a quantitative model that describes the effect of grain size on the sensitivity of metal-oxide gas sensors with nanosized grains ($D < 2L$). The model is applied for simulations of the sensitivity of nanocrystalline SnO_2 gas sensors as a function of the grain size.

Present address: Crystal Physics and Electroceramics Laboratory, Department of Materials Science & Engineering, MIT, Cambridge MA 02139, USA.

*To whom all correspondence should be addressed. E-mail: avner@mit.edu

2. Model

Under conditions of $D < 2L$ the energy bands are nearly flat and there are no barriers for inter-crystallite charge transport [5]. Thus, the electrical conductivity (σ) is proportional to the effective carrier concentration (n_{eff}) in the crystallites

$$\sigma \propto n_{eff} = \frac{1}{V}\int_V n(r)\,dV, \tag{1}$$

where V is the volume of the crystallite and $n(r)$ the local carrier concentration at a distance r from its center. $n(r)$ is a function of the electrostatic potential at point r

$$n(r) = N_D \exp[-\phi(r)], \tag{2}$$

where N_D is the doping level and $\phi \equiv -q\varphi/kT$ is the reduced potential (q is the elementary electron charge, φ is the electrostatic potential, k is Boltzmann's constant, and T is the temperature). To simplify the problem we assume that the sensor material can be treated

approximately as a three-dimensional net of interconnected spherical crystallites with radius R ($D = 2R$ is the diameter, or in other words the grain size).

In order to calculate n_{eff} one should know the shape of the potential barrier $\phi(r)$ as a function of r. This can be derived by solving Poisson's equation (with the appropriate boundary conditions) and the charge neutrality condition. Poisson's equation in spherical coordinates is written

$$\frac{1}{r^2}\frac{\partial}{\partial r}\left(r^2\frac{\partial \phi}{\partial r}\right) = \frac{1}{L_D^2}\{1 - \exp[-\phi(r)]\}, \qquad (3)$$

where $L_D = (\varepsilon kT/q^2 N_D)^{1/2}$ is the Debye length and ε the dielectric constant. Due to their symmetry the electric field must vanish at the center of the crystallites, therefore the first boundary condition is $\partial\phi/\partial r = 0$ at $r = 0$. The second boundary condition can be set as $\phi = \phi_0$ at $r = 0$, where ϕ_0 should be obtained by solving the electroneutrality condition as described below. Analytical solutions of Eq. (3) can be obtained for two limiting cases: for weak potential ($\phi \ll 1$) and for strong potential ($\phi \gg 1$). Under weak potential conditions $(1 - e^{-\phi}) \approx \phi$ and the solution is

$$\phi(r) = \phi_0 \frac{\sinh(r/L_D)}{(r/L_D)}. \qquad (4)$$

Under strong potential conditions $(1 - e^{-\phi}) \approx 1$ and the solution is

$$\phi(r) = \phi_0 + \frac{1}{6}\left(\frac{r}{L_D}\right)^2. \qquad (5)$$

In order to calculate the potential ϕ_0 at the center of the grains one should solve the charge balance equation

$$\int_V [N_D - n(r)]\, dV = 4\pi R^2 N_t^-, \qquad (6)$$

where N_t^- is the density of occupied surface states (filled traps) at the surface. In the case of chemoresistive metal-oxide gas sensors these states are associated with chemisorbed adions, and therefore N_t^- and σ are sensitive to the ambient gas composition [1]. Equation (6) merely says that the number of electrons withdrawn from the crystallite is equal to the number of electrons trapped on its surface, thus it describes the electroneutrality condition.

The trapped charge density N_t^- depends on the total density of both occupied and unoccupied states (N_t), and on the energy level of these states (E_t) with respect to the Fermi energy (E_F) at the surface,

$$N_t^- = \frac{N_t}{1 + 2\exp[(E_t - E_F)/kT]_{r=R}}. \qquad (7)$$

It is noted that $(E_t - E_F)_{r=R} = (E_t - E_F)_{\phi=0} + kT\phi_s$, where $\phi_s \equiv \phi\ (r = R)$ is the surface potential. Therefore, N_t^- depends on ϕ_0 via Eqs. (4) or (5). Thus, the left-hand-side and the right-hand-side of Eq. (6) are both functions of ϕ_0, which can be determined univocally by solving Eq. (6) numerically. Subsequently, the shape of the potential barrier $\phi(r)$ is readily obtained by substituting ϕ_0 into Eqs. (4) or (5), depending on whether $\phi_0 < 1$ or $\phi_0 > 1$, respectively. Then, the effective carrier concentration (n_{eff}) can be calculated via Eq. (1). In order to examine the effect of the ambient gas composition on the electrical conductivity these calculations should be carried out as a function of the surface state density (N_t), which is largely controlled by surface interactions between the sensor and the gas phase [6].

3. Numerical Simulations

Figure 1 depicts the effective carrier concentration as a function of the surface state density for SnO_2 with $N_D = 1 \times 10^{17}$ cm^{-3} and various grain sizes at $T = 600$ K. The corresponding Debye length is $L_D = 18.5$ nm. The energy level of the trapping states, E_t, was taken to lie 1 eV below the conduction band

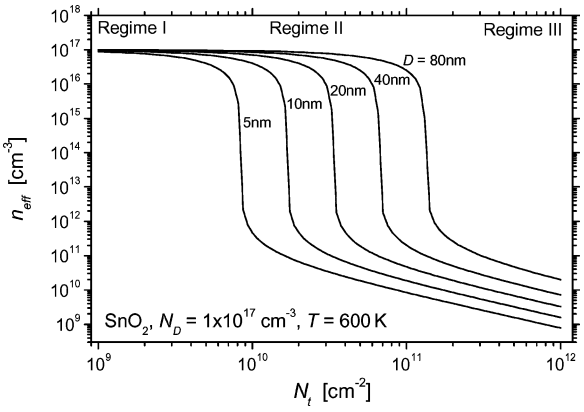

Fig. 1. The effective carrier concentration as a function of the surface state density for SnO_2 with various grain sizes as indicated in the figure.

edge at the surface. This value corresponds to the energy level of oxygen chemisorbates on SnO_2 [7]. Different gas species might have different electron affinities and therefore the corresponding energy level could vary from one gas to another.

The effective carrier concentration n_{eff} was calculated according to the computational method described above. Three characteristic regimes can be distinguished in Fig. 1, and the transition from one regime to another depends on the grain size. In the first regime (regime I), which is at low surface state densities, the effective carrier concentration decreases rather moderately with increasing surface state densities. But when the surface state density reaches a critical value $N_{t,crit}$ there is a sharp drop in the carrier concentration by several orders of magnitude. This drop occurs in the second regime (regime II) of the n_{eff} vs. N_t curves. One can see in Fig. 1 that with increasing grain sizes the transition from regime I to regime II shifts to higher surface state densities, or in other words the larger is the grain size the higher is $N_{t,crit}$. At higher surface state densities ($N_t > N_{t,crit}$), that is in the third regime (regime III), the carrier concentration decreases rather moderately with increasing surface state densities.

In order to gain additional insight into the behavior of n_{eff} as a function of N_t, Fig. 2 plots the trapped charge density N_t^- (occupied surface states) as a function of the surface state density N_t (both occupied and unoccupied states) as obtained form the simulations depicted in Fig. 1. One can see that below the critical point ($N_t < N_{t,crit}$) nearly all states are occupied and therefore$N_t^- \approx N_t$. This is because at low surface state densities the surface potential (ϕ_s) is small,

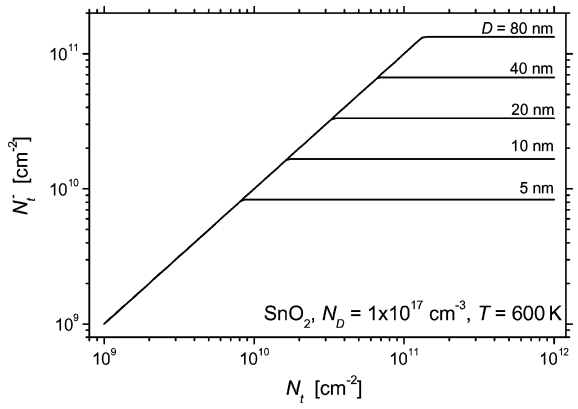

Fig. 2. The trapped charge density (occupied states) as a function of the surface state density (occupied and unoccupied states).

and since the states lie deep below the Fermi energy the occupation probability is close to unity. But when the critical point is reached, i.e. when $N_t = N_{t,crit}$, the surface potential increases considerably and consequently E_t shifts upwards and it almost levels with E_F. As a result, the occupation probability decreases and the trapped charge density (N_t^-) saturates and it hardly changes beyond this point. The simulations indicate that the saturation occurs when $N_t = N_{t,crit} = DN_D/6$ and $N_t^- \approx DN_D/6$, that is when nearly all electrons are trapped at the surface ($D/6$ is the volume to surface ratio of spherical crystallites with grain size D).

It should be noted that N_t^- still slightly grows with N_t even beyond the critical point ($N_t > N_{t,crit}$), but these very small changes cannot be resolved in Fig. 2. However, they still lead to quite considerable changes in the effective carrier concentration, as shown in Fig. 1 (regime III). This is because the effect of the variations in the trapped charge density on the carrier concentration are multiplied by the surface to volume ratio, $6/D$, which is a very large factor in nanocrystalline materials.

4. Discussion

The simulations depicted in Fig. 1 show that the grain size has a crucial effect on the effective carrier concentration, thus on the electrical conductivity. In this section we shall elaborate the effect of grain size on the sensitivity to gases, but before doing that we should first define the main sensor characteristics: the *output response signal* ($\Re$) and the *sensitivity* (S). The *output response signal*, $\Re = \sigma/\sigma_0$, is the ratio of the conductivity measured during exposure to the test gas (σ) and the conductivity measured under the baseline conditions (σ_0), which normally means in clean air. A plot of the response signal as a function of the gas composition (or in other words the concentration C of the test gas in air) is the sensor's *response curve*, and the *sensitivity* is defined as the slope of this curve, $S = \partial\Re/\partial C$ [8].

In the case of chemo-resistive metal-oxide gas sensors the ambient gas composition modifies the trapped charge density N_t^-. This is largely due to interactions between the test gas (which is normally a reducing gas such as CO, H_2, hydrocarbons and various volatile organic compounds) and pre-adsorbed oxygen adions ($O_{(ad)}^-$) [1]. For instance, CO molecules interact with pre-adsorbed oxygen adions and oxidize to CO_2 molecules, $CO_{(g)} + O_{(ad)}^- \rightarrow CO_{2(g)} + e_{cb}^-$ [9]. As a

result, the chemisorption-induced trapped charge density decreases, and the electrons that were trapped in the oxygen adions that interacted with the CO molecules are now liberated and return as free electrons (e^-_{cb}) to the conduction band. Thus, N_t^- depends on the gas concentration (C). Deriving the exact relationship between N_t^- and C is beyond the scope of this work, and we refer to Ref. [10] for further details. Instead, following Vlachos & Papadopoulos [11] we embrace a more fundamental approach and define the *normalized sensitivity* $\hat{S} = -\partial(\sigma/\sigma_0)/\partial(N_t^-/N_{t,0}^-)$, where $N_{t,0}^-$ is the trapped charge density in clean air, that is under the baseline conditions. The minus sign is due to the fact that N_t^- decreases when C increases. This approach circumvents the need to know the exact relationship between N_t^- and C, which may vary from one gas to another. Thus, it enables to deal exclusively with the transducer function of the sensor without having to consider the specific details of the chemical reactions that control its receptor function [1]. The underlying rationale is that a given change in the ambient gas composition should always lead to the same modification in the normalized trapped charge density, $N_t^-/N_{t,0}^-$.

Using the data from the simulations presented in the previous section, Fig. 3 depicts the normalized response curves, wherein $\Re = \sigma/\sigma_0 = n_{eff}/n_{eff,0}$ is plotted as a function of the normalized trapped charge density $N_t^-/N_{t,0}^-$. $n_{eff,0}$ and $N_{t,0}^-$ are the corresponding values when $N_t = 10^{12}$ cm^{-2}. One can see that the response signal increases linearly with decreasing values of the normalized trapped charge density. This implies that the nonlinearity of the non-normalized response curves ($\Re$ vs. C) of metal-oxide gas sensors, which is

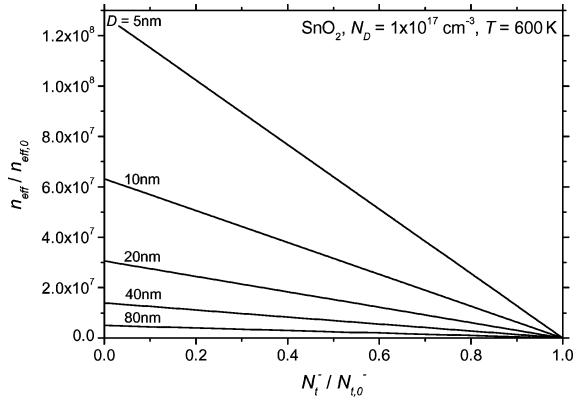

Fig. 3. The normalized response curve according to the simulations presented in Figs. 1 and 2.

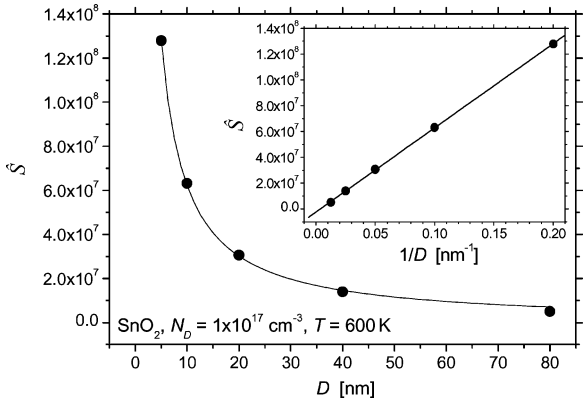

Fig. 4. The normalized sensitivity, $\hat{S} = -\partial(n_{eff}/n_{eff,0})/\partial(N_t^-/N_{t,0}^-)$, as a function of the grain size.

often reported in the literature, probably arises from the nature of the chemical interactions between the sensor and the gas phase rather than from the transduction mechanism that transforms these interactions into electrical signals (conductivity change). Indeed, chemisorption of reactive gases on SnO_2 and other semiconducting metal-oxides usually demonstrates a nonlinear behavior [6, 10].

Figure 3 also shows that the slope of the normalized response curves increases in magnitude when the grain size decreases, or in other words the normalized sensitivity $\hat{S}$ increases when D decreases. Specifically, $\hat{S}$ is found to be proportional to $1/D$, as shown in Fig. 4. This important result suggests that the sensitivity is proportional to the surface to volume ratio, which is equal to $6/D$ for spherical crystallites.

It is noteworthy that the response signal of nanocrystalline SnO_2 gas sensors is typically of the order of $10^1 \div 10^2$ for gas concentrations up to some hundreds ppm [1, 3], whereas according to Fig. 3 the response signal can be as high as $\sim 10^7$ when the normalized trapped charge diminishes by about $10 \div 20\%$. This implies that in practice the gas-induced modifications in the trapped charge density are much lower than that, reaching perhaps some ppm, namely $(N_{t,0}^- - N_t^-)/N_{t,0}^- \approx 10^{-6}$. In this case our simulations yield $n_{eff}/n_{eff,0} = 129$ for the most sensitive sensor (with $D = 5$ nm), which is a reasonable value for SnO_2 gas sensors with similar characteristics [1, 3]. Thus, the gas-induced modifications in the trapped charge density, which are mostly related to the receptor function of the sensor, are probably quite low under the normal operating conditions of gas sensors (that is when

the gas concentration is of the order of some tens or hundreds ppm). But it turns out from our simulations that these small variations are greatly amplified by the transducer function of the sensor, so that the output response signal is quite high eventually. Moreover, the results depicted in Fig. 4, which demonstrate that the normalized sensitivity is proportional to $1/D$, suggest that the amplification power of the sensor depends on its surface to volume ratio.

5. Summary and Conclusions

The effective carrier concentration in nanosized SnO_2 crystallites was calculated as a function of the surface state density for various grain sizes between 5 and 80 nm. The simulations demonstrated a sharp decrease in the carrier concentration when the surface state density reaches a critical value that corresponds to a condition of fully depleted grains, that is when nearly all the electrons are trapped at the surfaces of the crystallites. This critical value is proportional to the grain size D.

Assuming that the variations in the surface state density are induced by chemisorption and surface interactions with the gas phase, these simulations enable to evaluate the normalized response curves of nanocrystalline SnO_2 gas sensors. It was found that the conductivity increases linearly with decreasing trapped charge densities. This implies that the sensor's transducer function is linear. Thus, the nonlinearity in the overall response function (namely, the conductivity as a function of the test gas concentration) of SnO_2 gas sensors, which is often reported in the literature, seems to arise from the surface interactions between the sensor and the gas phase, or in other words from the sensor's receptor function.

Our simulations indicate that even very small ($\sim$1 ppm) variations in the trapped charge density can induce significant changes in the sensor's conductivity when the grain size is small ($\sim$5 nm). Namely, the gas-induced modifications in the trapped charge density are greatly amplified by the sensor's transduction function. Furthermore, the calculations show that the (normalized) sensitivity is proportional to $1/D$, which suggests that the amplification power is proportional to the surface to volume ratio of the sensor material. This result has important implications on the design of chemo-resistive metal-oxide gas sensors for optimizing their gas sensitivity.

Acknowledgments

A. R. would like to thank the Israeli Ministry of Science for the Eshkol fellowship and the Israeli Council for Higher Education for the VATAT fellowship. Y. K. would like to thank the Fund for the Promotion of Research at the Technion for partial support.

References

1. N. Yamazoe, *Sensors and Actuators B*, **5**, 7 (1991).
2. Y. Shimizu and M. Egashira, *MRS Bulletin*, **24**, 18 (1999).
3. S. Seal and S. Shukla, *JOM*, **54**, 35 (2002).
4. C. Xu, J. Tamaki, N. Miura, and N. Yamazoe, *Journal of The Electrochemical Society of Japan*, **58**, 1143 (1990); *Sensors and Actuators B*, **3**, 147 (1991).
5. J.W. Orton and M.J. Powell, *Reports on Progress in Physics*, **43**, 1263 (1980).
6. A. Rothschild and Y. Komem, *Sensors and Actuators B*, **93**, 362 (2003).
7. V. Lantto and P.R. Romppainen, *Surf. Sci.*, **192**, 243 (1987).
8. A. D'Amico and C. Di Natale, *IEEE Sensors Journal*, **1**, 183 (2001).
9. H. Windischmann and P. Mark, *Journal of The Electrochemical Society*, **126**, 627 (1979).
10. N. Barsan and U. Weimar, *Journal of Electroceramics*, **7**, 143 (2001).
11. D.S. Vlachos, C.A. Papadopoulos, and N.J. Avaritsiotis, *Journal of Applied Physics*, **80**, 6050 (1996).